A new approach to three-phase asynchronous motor model for electric power system analysis

Laura Collazo Solar [1], Angel A. Costa Montiel[2], Miriam Vilaragut Llanes[3], Vladimir Sousa Santos[4]
[1-3]Centro de Investigaciones y Pruebas Electroenergéticas (CIPEL), Universidad Tecnológica de la Habana "José Antonio Echeverría" (Cujae), La Habana, Cuba
[4]Energy Department, Universidad de la Costa, Barranquilla, Colombia

Article Info

Article history:

Received Aug 3, 2021
Revised Sep 23, 2021
Accepted Oct 1, 2021

Keywords:

Electrical power systems
Equivalent circuit
Load modeling
Mechanical load drive
Three-phase asynchronous motors
ZIP model

ABSTRACT

In this paper, a new steady-state model of a three-phase asynchronous motor is proposed to be used in the studies of electrical power systems. The model allows for obtaining the response of the demand for active and reactive power as a function of voltage and frequency. The contribution of the model is the integration of the characteristics of the mechanical load that can drive motors, either constant or variable load. The model was evaluated on a 2500 kW and 6000 V motor, for the two types of mechanical load, in a wide range of voltage and frequency, as well as four load factors. As a result of the evaluation, it was possible to verify that, for the nominal frequency and voltage variation, the type of load does not influence the behavior of the powers and that the reactive power is very sensitive to the voltage variation. In the nominal voltage and frequency deviation scenario, it was found that the type of load influences the behavior of the active and reactive power, especially in the variable load. The results demonstrate the importance of considering the model proposed in the simulation software of electrical power systems.

Corresponding Author:

Vladimir Sousa Santos
Energy Department
Universidad de la Costa
Calle 58 No.55-66, Barranquilla, Colombia
Email: vsousa1@cuc.edu.co

1. INTRODUCTION

The operation of electrical power systems (EPS) is commonly assessed through load flow, voltage stability, and short-circuit studies, among others. This is done with the help of software programmed with electromagnetic equations and mathematic models that simulate the behavior of the main components (i.e., generators, load, line, transformers, and machines) [1], [2]. Updating the load models commonly used in simulation programs of EPS is an imperative need today due to the increase in emerging smart grid technologies such as distributed generators, electric vehicles, and static power converters, among others. Modeling this type of load is difficult due to its time-varying and weather-dependent nature, as well as the lack of measurements [3].

The three-phase asynchronous motors (TAM) are one of the most important loads in EPS since it is estimated that there are around 300 million of this equipment installed in industries [4], representing the consumption of around 43 to 46% of energy electricity worldwide and between 60 and 70% of energy in industries [5]-[7]. Due to the importance of TAMs, they have been the subject of numerous studies focused mainly on the improvement of the technology to increase the level of efficiency [8], [9], on control strategies in the TAMs drive system to guarantee maximum operating efficiency [10]-[12] and on methods for estimating TAM operational efficiency [13], [14]

The importance of improving the modeling of TAMs in the simulation programs of EPS was evidenced by the blackout in the United States that occurred in 1996 and 2000 when millions of North Americans were without electricity for several hours [15]. In a study led by the "western electricity coordinating council," it was shown that the system in the affected area did not include the modeling of various TAMs and electronic loads, therefore, the behavior of the EPS could not be predicted correctly [16]-[18].

Normally, the TAM is represented as a constant power load, or constant impedance [3], [19]. Assuming constant active power may be acceptable in some cases but ignoring the variation of reactive power with voltage in TAM leads to significant errors. Neither has the behavior of the power consumed by the TAM been analyzed in the event of frequency deviations from its nominal value. Normally, in frequency stability studies, concentrated models of the loads are used, for which it is necessary to determine the so-called load-damping constant [2]. There are no concrete proposals in the literature to estimate this parameter in predominantly TAM loads.

According to CIGRE [20], there are two types of load models depending on the way to obtain their parameters. One way is based on measurements made in situ and, another way is based on the knowledge of the components of the loads and the development of models estimating the corresponding parameters. In the case of the TAM, the method based on measurements is impracticable because it requires laboratories where a considerable number of TAMs can be tested, both low and medium voltage and of different power and number of poles.

This paper aims to propose a new model of the TAM that allows its use in the analysis of EPS. The proposed model allows the analysis of the influence of the variation of voltage and frequency deviation, as well as the type of the mechanical load driven by the motor, on the active and reactive power consumption of the motors. The inclusion of the consideration of the type of mechanical load driven by the motor in the composite model is a novel aspect that can contribute to the improvement of the EPSs simulation software. Section 2 describes the state of the art of developed models of TAMs as load in the EPS. Section 3 explains the model with the equations and the sequential procedure for its application, while the explanation of the model is presented in section 4. In section 5 the conclusions of the article are discussed.

2. RESEARCH METHOD

2.1. State of the art of developed models of TAMs as load in the EPS.

Balanathan *et al*. [21] the approximate equivalent circuit shown in Figure 1 is proposed. In this case, the stator resistance and magnetization reactance are not considered. Neglecting the stator resistance does not generate a significant error, but not considering the magnetization reactance implies simplifying the main consumer of reactive power, which is unacceptable.

Where: P is the active power, Q is the reactive power, I is the current, V_1 is the voltage per phase, X_1 is the stator leakage reactance, X_2 is the rotor leakage reactance, R_2 is the rotor resistance, E is the electromotive force induced in the rotor, and s is the slip. Choi *et al*. [22] it is proposed to incorporate the equivalent circuit, as a model, in power system studies, as it appears in Figure 2, giving rise to the so-called "ZIP model with TAM ".

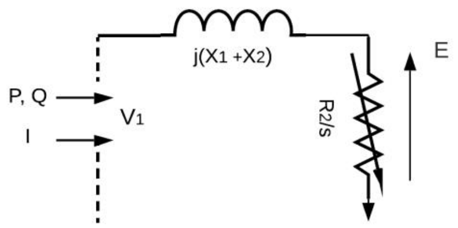

Figure 1. Approximate equivalent circuit of a TAM, proposed in the literature [21]

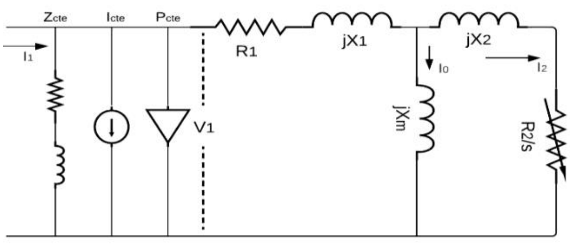

Figure 2. ZIP model with TAM [22]

Where: I_1 is the current per phase in the stator, Z is the impedance, R_1 is the stator resistance, X_m is the magnetizing reactance, I_0 is the current per phase of magnetization, and I_2 is the current per phase in the rotor. Aree [23] the equivalent circuit shown in Figure 3 is used to determine, during the execution of the load flow, the active and reactive power of the TAM load according to the voltage values calculated in successive iterations. This circuit is transformed by applying Thevenin's theorem [24] and with this, the active and reactive power is determined in each iteration. Certain input power is assumed (the work does not explain how to obtain this power from the TAM data and its load), and with it and the TAM parameters or with added parameters, the slip, and reactive power are determined. Core, mechanical and additional losses are not considered.

Wang *et al.* [15] a method based on a balance between the active and reactive powers supplied by the network and demanded by the TAM is used. From the solution of this balance, the active and reactive powers are determined in each iteration of the load flow program. The method assumes that the TAM output power is directly proportional to the square of the speed. Arif *et al*. [3] and Pereira *et al.* [25] the equivalent circuit shown in Figure 3 is also used. This circuit does not consider a parameter to represent the constant and additional losses.

The SimPowerSystem® of MatLab® [26] has a TAM model which requires the parameters and the mechanical output power of the TAM. The Power Factory® [27] proposes two methods to represent the steady-state model of the TAM in load flow studies:

- Slip Iteration (Slip Iteration AS). It is based on the exact equivalent circuit. The model equations are evaluated in a steady state. The user defines only the EPS input. By performing the iterations corresponding to the load flow, the slip and reactive power are determined.
- Constant PQ load. It is the classical method of representing the TAM.

Using the equivalent circuit directly as the model of the TAM, as proposed in the existing literature,
has the following disadvantages:

- It requires knowledge of all the parameters of the circuit. This information is not provided by almost any manufacturer and is complicated when working with several TAMs connected to the same bus, as is the case in almost all industries.
- It does not consider the effect of the type of load or mechanism driven by the TAM. Most TAMs drive pumps, compressors, or centrifugal fans, which are variable torque mechanisms whose slip varies with the voltage. This aspect is not considered in most of the methods proposed in the literature consulted, nor in the SimPowerSystem® or DigSilent PowerFactory® software.
- They do not consider the effect of frequency variation directly.
- The models required for power flow studies usually directly reflect the functional relationship of the active and reactive power consumed, with the voltage and frequency deviation around its nominal value.

The consideration of the variation of the frequency and the voltage in the operation of the TAM is an aspect that gains relevance in these times due to the increasing use of variable speed drives and of distributed generation sources that use non-linear elements [28]. The type of mechanical load that the motors drive is an important aspect that must be assessed as it determines their operating characteristics and active and reactive power demand from the EPS. About 55% of electric motors drive pumps and fans and 37% drive compressors and conveyors [29]. The relationship between speed and mechanical torque of pumps and fans is quadratic, and that of compressors and conveyors is constant. In other types of mechanical load driven by the motor such as mixers or extruders, the relationship between speed and torque is linear [4].

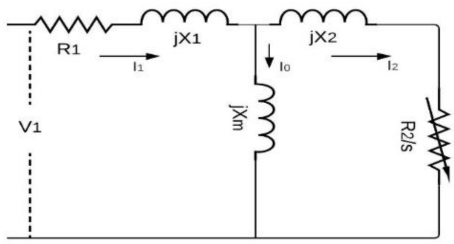

Figure 3. The equivalent circuit is proposed in the bibliography [23]

In summary, in EPS studies, TAM is represented as a purely electrical load of constant power or constant impedance or, at best, expressed by constant slip [17], [30], [31]. In TAM, the behavior of active and reactive power consumption to voltage and frequency depends on the type of mechanical load that drives and the load factor. In this work, these factors are considered.

2.2. Proposed model

Static load models have long been applied to represent static load components, such as resistive and lighting loads, and to estimate dynamic load components in EPSs [32]. These models are mainly used in the analysis of the equilibrium condition of EPS [33]. Static load models can be expressed as a polynomial or exponential model. The most used is the polynomial model defined as [2]:

$$P = P_0 \cdot \left[p_1 \cdot \left(\frac{V}{V_{base}}\right)^2 + p_2 \cdot \left(\frac{V}{V_{base}}\right) + p_3\right] \quad (1)$$

$$P_{pu} = p_1 \cdot V_{pu}{}^2 + p_2 \cdot V_{pu} + p_3 \quad (2)$$

$$Q = Q_0 \cdot \left[q_1 \cdot \left(\frac{V}{V_{base}}\right)^2 + q_2 \cdot \left(\frac{V}{V_{base}}\right) + q_3\right] \quad (3)$$

$$Q_{pu} = q_1 \cdot V_{pu}{}^2 + q_2 \cdot V_{pu} + q_3 \quad (4)$$

Where: (p_1, p_2, p_3) are the coefficients of the ZIP model for the active power, P_{pu} is the active power in p.u, P_0 is the active power at the base voltage, (q_1, q_2, q_3) are the coefficients of the ZIP model for the reactive power, V is the voltage, V_{base} is the base voltage, V_{pu} is the voltage in p.u, Q_0 is the reactive power at the base voltage, and Q_{pu} is the reactive power in p.u. The parameters (p1, p2, p3) and (q1, q2, q3) must meet the conditions:

$$p_1 + p_2 + p_3 = 1 \quad (5)$$

$$q_1 + q_2 + q_3 = 1 \quad (6)$$

As can be seen, these equations have three components: the first, proportional to the square of the voltage, corresponds to a constant impedance load, the second, proportional to the voltage, corresponds to a constant current load, and the third, as a constant term, corresponds to a constant power load. Because of this, this representation of the load is called the ZIP model (Z Impedance, I Current, P Power).
The equations of the polynomial model to take into account also the frequency variation are [3]:

$$P = P_0 \cdot \left[p_1 \cdot \left(\frac{V}{V_{base}}\right)^2 + p_2 \cdot \left(\frac{V}{V_{base}}\right) + p_3\right] \cdot (1 + K_{pf} \cdot \Delta f) \quad (7)$$

$$P_{pu} = \left(p_1 \cdot V_{pu}{}^2 + p_2 \cdot V_{pu} + p_3\right) \cdot (1 + K_{pf} \cdot \Delta f) \quad (8)$$

$$Q = Q_0 \cdot \left[q_1 \cdot \left(\frac{V}{V_{base}}\right)^2 + q_2 \cdot \left(\frac{V}{V_{base}}\right) + q_3\right] \cdot (1 + K_{qf} \cdot \Delta f) \quad (9)$$

$$Q_{pu} = \left(q_1 \cdot V_{pu}{}^2 + q_2 \cdot V_{pu} + q_3\right) \cdot (1 + K_{qf} \cdot \Delta f) \quad (10)$$

Where: K_{pf} is the coefficient of variation of the active power, K_{qf} is the coefficient of variation of the reactive power, and Δf is the deviation of the frequency from the nominal. The model can be represented schematically as shown in Figure 4.

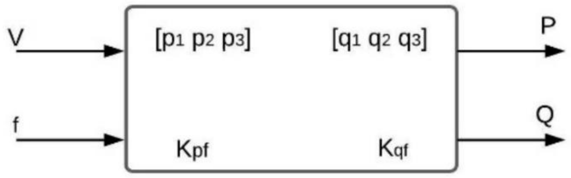

Figure 4. Schematic of the polynomial model of the TAM

where f is the frequency of the EPS.

2.2.1. Estimation of model parameters

In the application of the polynomial model, an important goal is to estimate the parameters of Figure 4 (i.e., p1, p2, p3, q1, q2, q3, Kpf, and Kqf). In this investigation, the exact equivalent circuit shown in Figure

5 was used applying the following methodology. With the datasheet or the data provided by the manufacturer, the circuit parameters are estimated, following the method explained in [34].

- Considering the characteristics of the driven mechanism and using the method explained in the next section, the voltage is varied in a suitable range at the nominal frequency. For each voltage value, the circuit is solved, and the active and reactive input power is determined. At the same time, the characteristic model that relates the powers to the voltage per unit is obtained.
- The parameters in (2) and (4) are obtained using a curve fitting method.
- Repeat step 2 but varying the frequency deviation at the nominal voltage.
- The parameters in (7) and (9) are obtained using a curve fitting method.

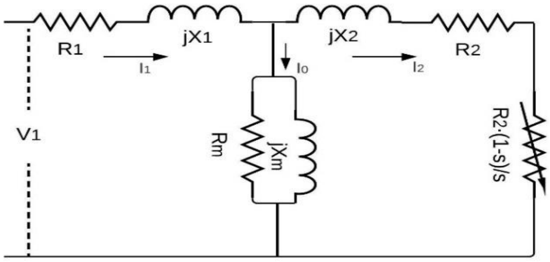

Figure 5. Exact equivalent circuit of the TAM [27]

where f is the frequency of the EPS.

2.2.2. Consideration of the influence of mechanical load driven by the TAM

Next, how the proposed method considers the influence of the type of mechanical load that drives the TAM on the behavior of the active and reactive power demand and the voltage and frequency of the EPS is explained. The two types of mechanical load that can drive ATMs are:

– Constant torque loads.

$$T_{mec} = T_c \tag{11}$$

– Variable torque loads.

$$T_{mec} = T_0 + T_1 \cdot n + T_2 \cdot n^2 \tag{12}$$

where: T_{mec} is the mechanical torque, T_c is the torque at the intersection point of the characteristic curve of the motor and the load, (T_o, T_1, T_2) are the variable torque model coefficients, and n is the speed of the rotor shaft. The equation of electromagnetic torque produced by the TAM, depending on the parameters of the equivalent circuit, is [24]:

$$T_{em} = \frac{3 \cdot {V_1}^2}{\omega_s} \cdot \frac{R_2}{s \cdot \left[\left(R_1 + \frac{R_2}{s}\right)^2 + (X_1 + X_2)^2\right]} \tag{13}$$

where T_{em} is the electromagnetic torque and ω_s is the angular synchronic velocity.
In the steady-state operating zone of the TAM, the following is fulfilled:

$$\frac{R_2}{s} >> R_1 \tag{14}$$

$$\frac{R_2}{s} >> X_1 + X_2 \tag{15}$$

Considering (14) and (15), (13) can be written as:

$$T_{em} = \frac{3 \cdot {V_1}^2}{\omega_s \cdot R_2} \cdot s \tag{16}$$

Considering that 3, ωs, and R2 are constants, (16) can be written as:

$$T_{em} = k_1 \cdot V_1^2 \cdot s \quad (17)$$

The constant K1 can be expressed as:

$$k_1 = \frac{T_{mecn}}{V_{1n}^2 \cdot s_n} \quad (18)$$

Where K_1 is the constant used for the electromagnetic torque model as a function of variable voltage and constant frequency, T_{mecn} is the nominal mechanical torque and V_{1n} is the nominal voltage per phase.
The slip is related to speed through:

$$n = n_s \cdot (1 - s) \quad (19)$$

In the case of constant torque load, (11) is used, equating the mechanical torque with that of the load. If the voltage decreases, the slip must increase so that the torque remains constant and vice versa. This makes it possible to assume that the product (s·V12) remains constant (see (17)) and then:

$$k_v = V_1^2 \cdot s \quad (20)$$

Where K_v is the constant used for the electromagnetic torque model as a function of variable voltage and constant frequency.

The algorithm to be programmed is based on assuming a load torque value for which the corresponding Kv is calculated and then varying the voltage from 80% to 120% of the nominal one. For each voltage value, calculate the active power and the reactive input power. This makes it possible to obtain the characteristics of these two variables as a function of the voltage.

In the case of variable torque, it should be noted that varying the slip also changes the torque as the speed n = ns (1-s) varies.
where n_s is the synchronic speed.
For the variable torque, it is satisfied that:

$$T_c = T_0 + T_1 \cdot n + T_2 \cdot n^2 \quad (21)$$

$$T_c = T_0 + T_1 \cdot n_s \cdot (1 - s) + T_2 \cdot {n_s}^2 \cdot (1 - 2 \cdot s + s^2) \quad (22)$$

$$T_c = (T_0 + T_1 \cdot n_s + T_2 \cdot {n_s}^2) - (T_1 \cdot n_s + 2 \cdot T_2 \cdot {n_s}^2) \cdot s + T_2 \cdot {n_s}^2 \cdot s^2 \quad (23)$$

Substituting (16) in (18) it is obtained that:

$$k_1 = \frac{3}{\omega_s \cdot R_2} \quad (24)$$

Equation (17) and (23) and making some transformations are obtained:

$$0 = (T_0 + T_1 \cdot n_s + T_2 \cdot {n_s}^2) - \left(T_1 \cdot n_s + 2 \cdot T_2 \cdot {n_s}^2 + K_1 \cdot {V_1}^2\right) \cdot s + T_2 \cdot {n_s}^2 \cdot s^2 \quad (25)$$

$$A_0 = (T_0 + T_1 \cdot n_s + T_2 \cdot {n_s}^2) \quad (26)$$

$$A_1 = \left(T_1 \cdot n_s + 2 \cdot T_2 \cdot {n_s}^2 + K_1 \cdot {V_1}^2\right) \quad (27)$$

$$A_2 = T_2 \cdot {n_s}^2 \quad (28)$$

Where A_0, A_1, A_2 are variable load and constant frequency model coefficients.
The equation that gives the slip value for each voltage value is:

$$0 = A_0 - A_1 \cdot s + A_2 \cdot s^2 \quad (29)$$

This equation has two solutions, one of them is within the range of possible slip values (0 <s <1) and the other solution exceeds this value by more than 10 times and is therefore not considered. With the slip value given by these equations, the equivalent circuit is solved for each of the voltage values and the values of active power and reactive power are calculated, as it was done in the constant torque load.
In the case of frequency variation, in (8) and (10) the voltage is made in per unit equal to 1 and is obtained:

$$P_{pu} = (1 + K_{pf} \cdot \Delta f) \quad (30)$$

$$Q_{pu} = (1 + K_{qf} \cdot \Delta f) \quad (31)$$

Frequency variation implies a new value of synchronous speed and requires a new way of determining torque from:

$$T_{em} = \frac{3 \cdot {V_1}^2}{\omega_s \cdot R_2} \cdot \frac{\omega_s - \omega_r}{\omega_s} \quad (32)$$

$$T_{em} = \frac{3}{R_2} \cdot \left(\frac{V_1}{\omega_s}\right)^2 \cdot (\omega_s - \omega_r) \quad (33)$$

The term V1/ωs expressed per unit coincides with the magnetic flux per unit (V/f=k) because it is proportional to it. The following term is then defined as “Equivalent Flux”.

$$\phi_{eq} = \frac{V_1}{\omega_s} \quad (34)$$

Substituting (34) in (33) it is obtained that:

$$T_{em} = K_\omega \cdot {\phi_{eq}}^2 \cdot (\omega_s - \omega_r) \quad (35)$$

Where K_ω is the constant used for the electromagnetic torque model as a function of variable voltage and frequency, ϕ_{eq} is the equivalent flux and ω_r is the angular shaft speed. The constant Kω is calculated as:

$$K_\omega = \frac{T_{mecn}}{{\phi_{eqn}}^2 \cdot (\omega_{sn} - \omega_{rn})} \quad (36)$$

Where ϕ_{eqn} is the nominal equivalent flux, ω_{rn} is the nominal angular shaft speed and ω_{sn} is the nominal angular synchronic velocity. In the case of constant torque load, frequency values are expressed as:

$$f = f_n + \Delta f \quad (37)$$

Where fn is the nominal frequency.
This frequency is substituted in:

$$\omega_s = \frac{2 \cdot \pi \cdot f}{p} \quad (38)$$

Where p is the number of poles of the motor.
This equation and (34) with the nominal parameters are replaced in (36). The reactance values are changed according to the frequency. With these values and the other TAM parameters, the equivalent circuit is solved, and the active power and the reactive power are calculated. If the load is of variable torque, (23) is (35) and the speed in rpm (n) is replaced by the speed in rad/s (ωs) applying (39).

$$n_s = \omega_s \cdot \left(\frac{30}{\pi}\right) \quad (39)$$

$$0 = \left(T_0 + T_1 \cdot \left(\frac{30}{\pi}\right) \cdot \omega_s + T_2 \cdot \left(\frac{30}{\pi}\right)^2 \cdot {\omega_s}^2\right) - \left(K_\omega \cdot {\phi_{eq}}^2 \cdot \omega_s + T_1 \cdot \left(\frac{30}{\pi}\right) \cdot \omega_s + 2 \cdot T_2 \cdot \left(\frac{30}{\pi}\right)^2 \cdot \omega_s^2\right) \cdot s + \left(T_2 \cdot \left(\frac{30}{\pi}\right)^2 \cdot \omega_s^2\right) \cdot s^2 \quad (40)$$

$$B_0 = \left(T_0 + T_1 \cdot \left(\frac{30}{\pi}\right) \cdot \omega_s + T_2 \cdot \left(\frac{30}{\pi}\right)^2 \cdot {\omega_s}^2\right) \quad (41)$$

$$B_1 = \left(K_\omega \cdot {\phi_{eq}}^2 \cdot \omega_s + T_1 \cdot \left(\frac{30}{\pi}\right) \cdot \omega_s + 2 \cdot T_2 \cdot \left(\frac{30}{\pi}\right)^2 \cdot \omega_s^2\right) \quad (42)$$

$$B_2 = \left(T_2 \cdot \left(\frac{30}{\pi}\right)^2 \cdot \omega_s^2\right) \quad (43)$$

Where (B_0, B_1, B_2) are the variable load and frequency model coefficients. In (40) is then like:

$$B_0 - B_1 \cdot s + B_2 \cdot s^2 = 0 \quad (44)$$

Solving this second-degree equation, two solutions are obtained, the smallest ($0 < s < 1$) is valid because it corresponds to the normal values of slip in the TAM. The rest of the procedure is the same as for a constant torque load.

3. RESULTS AND DISCUSSIONS

– Application of the method to a case study

To illustrate the method, the TAM of the feeding pump of a thermal power plant of 2500 kW; 6000 V; 2 poles and 60 Hz is selected, whose data is provided by the manufacturer, and parameters calculated from these data, appear in [34]. To determine the characteristics of active and reactive power as a function of voltage for both constant and variable torque, an operating point at a nominal voltage corresponding to 75% of the nominal load was assumed in both cases, at which the active power consumed is P=1817 kW and the reactive Q=1134 kVAr. For this, a MATLAB [26] program was used with the algorithm described in a previous section.

Figure 6 (a) shows the characteristic of active power as a function of voltage and in Figure 6 (b) the characteristic of reactive power as a function of voltage at nominal frequency. In both cases for a constant torque load and a variable torque load. The characteristics vary very little with the type of load. It is only noticeable in the active power characteristic, for voltage values are far from the nominal one.

It is also analyzed how the consumption of active and reactive power varies as a function of the voltage when the mechanical load of the TAM also varies, both for constant and variable torque load at nominal frequency. Figures 7 (a)-(b) shows the characteristics of active and reactive power as a function of voltage. In this case, the torque loads with constant and variable characteristics have the same behavior.

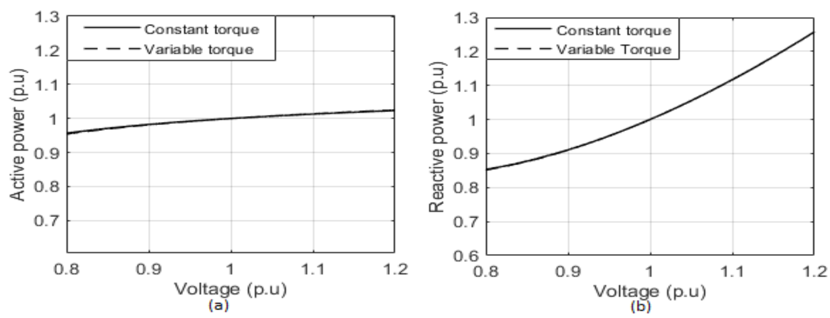

Figure 6. These figures are; (a) characteristic of active power as a function of the voltage, (b) characteristic of reactive power as a function of the voltage

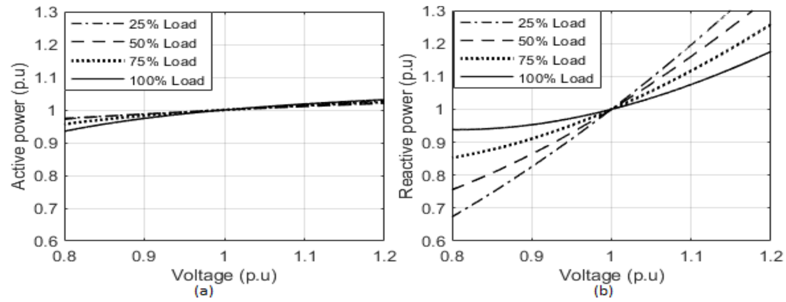

Figure 7. Characteristics of; (a) active power and (b) reactive power as a function of voltage at different load factors for constant and variable torque load

It is observed that the higher the load, the greater the variation of the active power with the voltage and the lower the reactive power. It can also be noted that, in both cases, the lower the load, the linearity of the characteristic increases. Using the Basic Fitting option of MATLAB [26], the parameters corresponding to the voltage for the model are given by (2) and (4) were determined and appear in Table 1 for the case of variable torque. To determine the characteristics of active and reactive power as a function of the frequency deviation for both constant torque and variable torque, an operating point at a nominal voltage corresponding to 75% of the nominal load was assumed in both cases, at which the power consumed is P = 1817 kW and Q = 1134 kVAr.

Table 1. Model parameters for variable torque load, at different load factors, and nominal frequency

Parameters	100 %	75 %	50 %	25 %
p1	-0.44	-0.28	-0.13	0.0046
p2	1.2	0.74	0.39	0.13
p3	0.28	0.53	0.74	0.87
q1	1.3	1.3	1.2	1.1
q2	-2.1	-1.7	-1	-0.31
q3	1.7	1.3	0.78	0.21

Figures 8 (a)-(b) shows the active power and reactive power characteristics as a function of the frequency deviation in both cases, for a constant torque load and a variable torque load. As can be seen in Figure 8 the active power characteristics as a function of the frequency deviation from the nominal, are linear with a much greater slope in the case of variable torque loads. However, the variation in reactive power is practically negligible. This behavior explains the advantage of using variable speed drives in this type of mechanical load driven by the motor for saving electrical energy [8], [35]. Next, the variation of the active and reactive power consumption is analyzed as a function of the frequency deviation at nominal voltage, when the load factor of the TAM also varies. Figures 9 (a)-(b) shows the variation for constant torque loads and Figure 10 (a)-(b) shows for variable torque loads. In both cases, the active power is represented in Figures 9 (a), and 10 (a) then the reactive power in Figures 9 (b), and 10 (b).

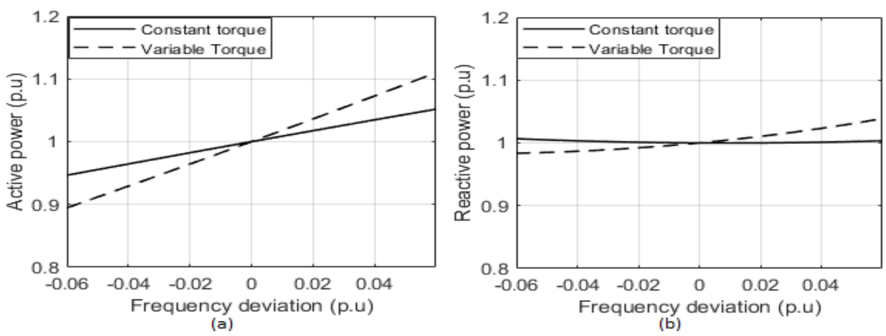

Figure 8. Characteristic of; (a) active power and (b) reactive power as a function of frequency variation

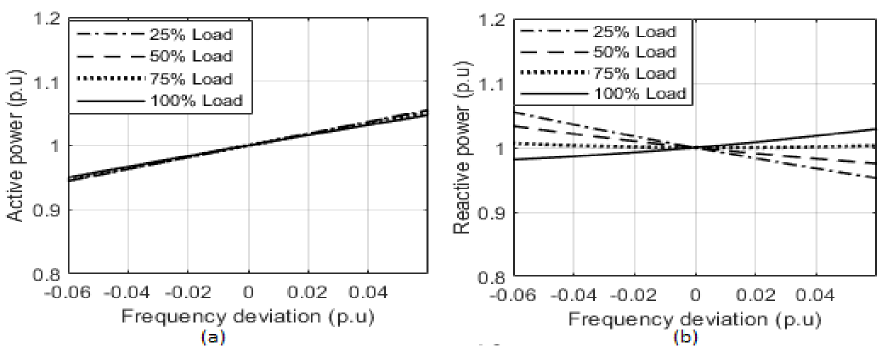

Figure 9. Characteristics of; (a) active power and (b) reactive power as a function of frequency variation at different load factors for constant torque load

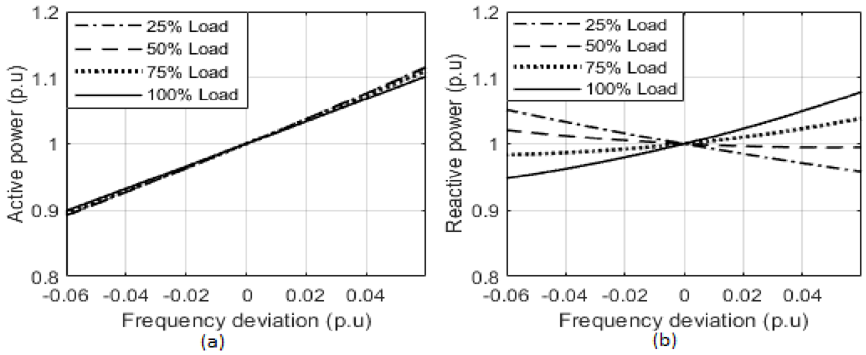

Figure 10. Characteristics of; (a) active power and (b) reactive power as a function of frequency variation at different load factors for variable torque load

The active power characteristic as a function of the frequency deviation about the nominal is practically independent of the load factor, that is, it can be assumed that it only depends on the type of load. Regarding the reactive power characteristic, it can still be assumed that the variation of the reactive power with the frequency deviation is practically negligible. Table 2 shows the parameters related to the frequency variation of the model of (15).

Table 2. Model parameters corresponding to frequency deviation, at different load factors, and nominal voltage

Parameters	100%	75%	50%	25%
Kpf (constant load)	0.81	0.88	0.92	0.93
Kpf (vatiable load)	2.5	2.6	2.8	2.8

4. CONCLUSION

According to the results, the following conclusions can be reached: The representation of the TAM through a quadratic polynomial is very suitable for its application in the analysis of EPS performance. The most convenient procedure to determine the model parameters is, based on the information provided by the manufacturer, to calculate the parameters of the exact equivalent circuit and, through it, to determine the active and reactive power characteristics as a function of the voltage and the frequency deviation around nominal one. With these characteristics, and applying some curve fitting method, determine the parameters of the proposed model. The model parameters depend, in general, on the type (constant torque or variable torque) and magnitude of the mechanical load driven by the TAM. The characteristics of active and reactive power as a function of the voltage do not depend on the type of load, but on its magnitude, while the characteristics as a function of the frequency deviation depend on the type of load but not on its magnitude. Active power varies much more with frequency in the case of a TAM that drives a variable torque mechanism than if the mechanism is constant torque. The reactive power consumed by the TAM varies very little as a function of the frequency deviation. Because of this, it is proposed to disregard it.

REFERENCES

[1] J. J. Grainger and W. D. Stevenson, "Power system analysis," New York: McGraw Hill, 1994.
[2] P. S. Kundur, "Power System Stability and Control, Third Edition. McGraw Hill," Inc., 1993.
[3] A. Arif, Z. Wang, J. Wang, B. Mather, H. Bashualdo and D. Zhao, "Load Modeling-A Review," *IEEE Transactions on Smart Grid*, vol. 9, no. 6, pp. 5986-5999, 2018, doi: 10.1109/TSG.2017.2700436.
[4] M. J. S. Zuberi, A. Tijdink, and M. K. Patel, "Techno-economic analysis of energy efficiency improvement in electric motor driven systems in Swiss industry," *Applied Energy*, vol. 205, no. January, pp. 85-104, 2017, doi: 10.1016/j.apenergy.2017.07.121.
[5] Ç. Acar, O. C. Soygenc, and L. T. Ergene, "Increasing the Efficiency to IE4 Class for 5.5 kW Induction Motor Used in Industrial Applications," *International Review of Electrical Engineering*, vol. 14, no. 1, p. 67, 2019, doi: 10.15866/iree.v14i1.16307.
[6] E. C. Quispe, V. S. Santos, I. D. López, J. R. Gómez, and P. R. Viego, "Theoretical Analysis of the Voltage Unbalance Factor to Characterize Unbalance Problems in Induction Motors," *Int. Rev. Electr. Eng.*, vol. 16, no. 1, pp. 1-8, 2021, doi: 10.15866/iree.v16i1.18881.

[7] J. R. Gómez *et al*., "Assessment criteria of the feasibility of replacement standard efficiency electric motors with high-efficiency motors," *Energy*, vol. 239, p. 121877, 2022, doi: 10.1016/j.energy.2021.121877.

[8] A. De Almeida, J. Fong, C. U. Brunner, R. Werle, and M. Van Werkhoven, "New technology trends and policy needs in energy efficient motor systems - A major opportunity for energy and carbon savings," *Renewable and Sustainable Energy Reviews*, vol. 115, p. 109384, 2019, doi: 10.1016/j.rser.2019.109384.

[9] P. R. Viego, V. Sousa, J. R. Gómez, and E. C. Quispe, "Direct-on-line-start permanent-magnet-assisted synchronous reluctance motors with ferrite magnets for driving constant loads," *Int. J. Electr. Comput. Eng.*, vol. 10, no. 1, p. 651, 2020, doi: 10.11591/ijece.v10i1.pp651-659.

[10] A. Trianni, E. Cagno, and D. Accordini, "Energy efficiency measures in electric motors systems: A novel classification highlighting specific implications in their adoption," *Applied Energy*, vol. 252, p. 113481, 2019, doi: 10.1016/j.apenergy.2019.113481.

[11] J. C. Travieso-Torres *et al.*, "New Adaptive High Starting Torque Scalar Control Scheme for Induction Motors Based on Passivity," *Energies*, vol. 13, no. 5, p. 1-15, 2020, doi: 10.3390/en13051276.

[12] F. J. T. E. Ferreira and A. T. de Almeida, "Reducing Energy Costs in Electric-Motor-Driven Systems: Savings Through Output Power Reduction and Energy Regeneration," *IEEE Industry Applications Magazine*, vol. 24, no. 1, pp. 84-97, 2018, doi: 10.1109/MIAS.2016.2600685.

[13] C. P. Salomon, W. C. Sant'Ana, G. L. Torres, L. E. B. D. Silva, E. L. Bonaldi, and L. E. D. L. D. Oliveira, "Comparison among methods for induction motor low-intrusive efficiency evaluation including a new AGT approach with a modified stator resistance," *Energies*, vol. 11, no. 4, pp. 1-21, 2018, doi: 10.3390/en11040691.

[14] V. S. Santos, J. J. C. Eras, A. S. Gutierrez, and M. J. Cabello Ulloa, "Assessment of the energy efficiency estimation methods on induction motors considering real-time monitoring," *Measurement*, vol. 136, pp. 237-247, 2019, doi: 10.1016/j.measurement.2018.12.080.

[15] D. Wang, X. Yuan, and M. Zhang, "Power-Balancing Based Induction Machine Model for Power System Dynamic Analysis in Electromechanical Timescale," *Energies*, vol. 11, no. 2, pp. 161-164, 2018, doi: 10.3390/en11020438.

[16] D. Kosterev and D. Davies, "System model validation studies in WECC," *IEEE PES General Meeting*, 2010, pp. 1-4, doi: 10.1109/PES.2010.5589797.

[17] J. C. Sánchez, T. I. A. Olivares, G. R. Ortiz and D. Ruiz-Vega, "Induction motor static models for power flow and voltage stability studies," *IEEE Power and Energy Society General Meeting*, 2012, pp. 1-8, doi: 10.1109/PESGM.2012.6345618.

[18] B. T. Ooi, J. Guo and X. Wang, "Nonlinear negative damping caused August 10, 1996-WECC blackout," *IEEE Power & Energy Society General Meeting PESGM*, 2020, pp. 1-5, doi: 10.1109/PESGM41954.2020.9281819.

[19] J. V. Milanovic, K. Yamashita, S. Martínez Villanueva, S. Ž. Djokic and L. M. Korunović, "International Industry Practice on Power System Load Modeling," *IEEE Transactions on Power Systems*, vol. 28, no. 3, pp. 3038-3046, Aug. 2013, doi: 10.1109/TPWRS.2012.2231969.

[20] Z. Y. Dong, A. Borghetti, K. Yamashita, A. Gaikwad, P. Pourbeik, and J. V. Milanović, "CIGRE WG C4 . 065 Recommendations on Measurement Based and Component Based Load Modelling Practice," *CIGRE SC C4 2012 Hakodate Colloquium*, no. June 2014, pp. 1-6, 2012.

[21] R. Balanathan, N. C. Pahalawaththa, and U. D. Annakkage, "Modelling induction motor loads for voltage stability analysis," *International Journal of Electrical Power & Energy Systems*, vol. 24, no. 6, pp. 469-480, 2002, doi: 10.1016/S0142-0615(01)00059-X.

[22] B. K. Choi, H. D. Chiang, Y. Li, Y. T. Chen, D. H. Huang and M. G. Lauby, "Development of composite load models of power systems using on-line measurement data," *IEEE Power Engineering Society General Meeting*, 2006, pp. 8, doi: 10.1109/PES.2006.1709013.

[23] P. Aree, "Load flow solution with induction motor," *Songklanakarin J. Sci. Technol*, vol. 28, no. 1, pp. 157-168, 2006.

[24] S. D. Umans, "Fitzgerald and Kingsley's Electric machinery," 2014.

[25] L. Pereira, D. Kosterev, P. Mackin, D. Davies, J. Undrill and Wenchun Zhu, "An interim dynamic induction motor model for stability studies in the WSCC," *IEEE Transactions on Power Systems*, vol. 17, no. 4, pp. 1108-1115, 2002, doi: 10.1109/TPWRS.2002.804960.

[26] MATLAB, "MATLAB R2019a." 2019.

[27] DIgSILENT, "DIgSILENT PowerFactory 15.1.7 (x86)." 2014.

[28] S. Rönnberg and M. Bollen, "Power quality issues in the electric power system of the future," *The Electricity Journal*, vol. 29, no. 10, pp. 49-61, 2016, doi: 10.1016/j.tej.2016.11.006.

[29] M. Hasanuzzaman, N. A. Rahim, R. Saidur, and S. N. Kazi, "Energy savings and emissions reductions for rewinding and replacement of industrial motor," *Energy*, vol. 36, no. 1, pp. 233-40, 2011, doi: 10.1016/j.energy.2010.10.046.

[30] A. J. Collin, J. L. Acosta, B. P. Hayes, and S. Z. Djokic, "Component-based aggregate load models for combined power flow and harmonic analysis," *7th Mediterranean Conference and Exhibition on Power Generation, Transmission, Distribution and Energy Conversion*, 2010.

[31] J. Carmona-Sánchez and D. Ruiz-Vega, "Review of static induction motor models," *North American Power Symposium*, 2010, pp. 1-8, doi: 10.1109/NAPS.2010.5619613.

[32] H. Renmu, Ma Jin and D. J. Hill, "Composite load modeling via measurement approach," *IEEE Transactions on Power Systems*, vol. 21, no. 2, pp. 663-672, 2006, doi: 10.1109/TPWRS.2006.873130.

[33] E. O. Kontis *et al*., "Development of measurement-based load models for the dynamic simulation of distribution grids," *IEEE PES Innovative Smart Grid Technologies Conference Europe (ISGT-Europe)*, 2017, pp. 1-6, doi: 10.1109/ISGTEurope.2017.8260251.

[34] L. C. Solar, A. A. C. Montiel, M. V. Llanes, V. S. Santos, and A. C. Colina, "A new exact equivalent circuit of the medium voltage three-phase induction motor," *International Journal of Electrical and Computer Engineering*, vol. 10, no. 6, pp. 6164-6171, 2020, doi: 10.11591/ijece.v10i6.pp6164-6171.
[35] D. R. Q. Sarmiento, J. R. García, and W. M. López, "Methodology to Measure Electric Discharge Machining (EDM) Bearing Currents in Induction Motors with Supply from a Variable Speed Drive (VSD)," *INGE CUC*, vol. 9, no. 2, pp. 83-93, 2014.

BIOGRAPHIES OF AUTHORS

Laura Collazo Solar was born in Havana, Cuba, on November 30, 1989. Received a B.Sc. in Electrical Engineering from Universidad Tecnológica de la Habana José Antonio Echeverría, Cuba in 2013. M.Sc. in Electrical Engineering from Universidad Tecnológica de la Habana José Antonio Echeverría, Cuba in 2020. She has published papers in induction motors parameters identification and energy efficiency. Her area of interest includes electric machines and drives and energy efficiency. Email: lcollazo@electrica.cujae.edu.cu, ID Scopus: (57219323523), ID ORCID (0000-0003-1139-4917), ID Google Scholar: (Laura Collazo Solar).

Angel A. Costa Montiel was born in Havana, Cuba, on March 21, 1944. Received a B.Sc. in Electrical Engineering from University of Havana, Cuba in 1968. PhD. in Technical Sciences (Electrical Engineering) from Universidad Tecnológica de la Habana José Antonio Echeverría, Cuba, in 1987. He has published papers in high impact journals indexed in Scopus in induction motors parameters identification, vector control of electric motors and artificial intelligence application to control of electric machines and drives. His area of interest are simulation and control of electric machines and drives and energy efficiency. Email: aacm@electrica.cujae.edu.cu, ID Scopus: (25633619100), ID ORCID (0000-0002-5347-8257), ID Google Scholar: (Angel Alberto Costa Montiel).

Miriam Vilaragut Llanes was born in Cienfuegos, Cuba, on April 13, 1959. Received a B.Sc. in Electrical Engineering from Universidad Tecnológica de la Habana José Antonio Echeverría, Cuba in 1982. M.Sc. in Electrical Engineering from Universidad Tecnológica de la Habana José Antonio Echeverría, Cuba in 1982. PhD. in Technical Sciences (Electrical Engineering) from Universidad Tecnológica de la Habana José Antonio Echeverría, Cuba, in 2002. She has published articles on electric drive, renewable energy sources and capacity building in high impact journals indexed in Scielo, Scopus and Wos. Her area of interest includes electric drives, renewable energy sources, and electric power system. Email: miriamv@electrica.cujae.edu.cu, ID Scopus: (57219331318), ID ORCID (0000-0002-5453-1136), ID Google Scholar: (Miriam Vilaragut Llanes).

Vladimir Sousa Santos was born in Cienfuegos, Cuba, on November 21, 1980. Received a B.Sc. in Electrical Engineering from the Universidad Central de Las Villas, Cuba in 2004. M.Sc. in Energy Efficiency from Universidad Cienfuegos, Cuba in 2004. PhD. in Electrical Engineering from Universidad Central de Las Villas, Cuba, in 2014. He has published articles on induction motors, energy quality, and energy efficiency in high impact journals indexed in Scopus and Wos. His area of interest includes electric machines, power quality, and energy efficiency. Dr. Sousa is an IEEE Member. Email: vsousa1@cuc.edu.co, ID Scopus: (57219326150), ID ORCID (0000-0001-8808-1914), ID Google Scholar: (Vladimir Sousa Santos), ID Publons: (T-8233-2019).